EG0500274

Thermal Radiation Effects on Hydromagnetic Flow

M.M. Abdelkhalek
Nuclear Physics Department, Nuclear Research Centre, AEA, Cairo, Egypt

ABSTRACT

Numerical results are presented for the effects of thermal radiation, buoyancy and heat generation or absorption on hydromagnetic flow over an accelerating permeable surface. These results are obtained by solving the coupled nonlinear partial differential equations describing the conservation of mass, momentum and energy by a perturbation technique. This qualitatively agrees with the expectations, since the magnetic field exerts a retarding force on the free convection flow. A parametric study is performed to illustrate the influence of the radiation parameter, magnetic parameter, Prandtl number, Grashof number and Schmidt number on the profiles of the velocity components and temperature. The effects of the different parameters on the velocity and temperature profiles as well as the skin friction and wall heat transfer are presented graphically. Favorable comparisons with previously published work confirm the correctness of numerical results.

Key Words : Heat and Mass Transfer / Hydromagnetic Flow / Perturbation Technique

INTRODUCTION

The study of the dynamics of conducting fluid find applications in a variety of engineering problems, the one related to the cooling processes of nuclear reactors, and that related to the connected flow through a porous medium, since the geothermic region gases are electrically conducting and affected by a magnetic field. The effect radiation MHD flow and heat transfer problems have become more important industrially. At high operating temperature, radiation effect can be quite significant. Many processes in engineering areas occur at high temperatures and knowledge of radiation heat transfer becomes very important for the design of pertinent equipment. Nuclear power plants, gas turbines and the various propulsion devices for aircraft, missiles, satellites and space vehicles are examples of such engineering areas. In recent years, considerable progress has been made in the study of heat and mass transfer in magnetohydrodynamics flow due to its application in many devices, like the MHD power generator and Hall accelerator. The influence of a magnetic field on the flow of an electrically conducting viscous fluid with mass transfer and radiation absorption is also useful in planetary atmosphere research[(1)].

Ram et al[(2)] studied the heat and mass transfer of a viscous heat generating fluid with hall current. Jha and Prasad[(3)] investigated MHD free convection and mass transfer flow through a porous medium with heat source. Takhar et al[(4)] investigated the hydromagnetic convection flow of a heat generating fluid past a vertical plate with hall current and heat flux through a porous medium. Georgiou and Georgantpoulos[(5)] studied the mass transfer effects on the transient behavior of the asymptotic laminar boundary layer. Hydromagnetic flows and heat transfer have become more important in recent years because of many important applications such that in many metallurgical processes which involve cooling of continuous strips or filaments, these elements are drawn through a quiescent fluid. During this process, these strips are sometimes stretched. The properties of the final product depend to a great extent on the rate of cooling. This rate of cooling has been proven to be controlled and therefore, the quality of the final product by drawing such strips in an electrically conducting fluid subject to a magnetic field[(9)] Soundalgekar et. Al[(6)] used a finite difference method to investigate free convection effects on the Stokes problem for a vertical plate in a dissipative fluid with constant heat flux.

Ram[7] also used the finite difference method to solve the MHD Stokes problem for vertical plate with hall and ion slip currents. Chaturvedi [8]studied the flow of incompressible viscous fluid past an impulsively started infinite porous plate with variable suction. Many works have been reported on flow and heat transfer over a stretched surface in the presence of a magnetic field[9-20]. Takhar et al[21] studied the radiation effects on MHD free-convection flow of a gas past a semi-infinite vertical plate. Recently the radiation effect on heat transfer over a stretching surface was studied by Elbashbeshy[22].

The purpose of this work is to study the effect of thermal radiation and heat generation or absorption on hydromagnetic flow over an accelerating permeable surface. The coupled nonlinear partial differential equations are solved by the perturbation technique. The effects of the different parameters on the velocity and temperature profiles as well as the skin friction and wall heat transfer are presented graphically.

FORMULATION OF THE PROBLEM

Consider steady, laminar, viscous boundary-layer flow over an accelerating semi-infinite vertical permeable surface. A uniform magnetic field is applied in the horizontal direction that is normal to the surface. A temperature dependent heat source or sink is assumed to be present in the flow and that thermal radiation and buoyancy effects are significant. All fluid properties are assumed to be constant except the density in the body force term of the balance of linear momentum. The magnetic Reynolds number is assumed to be small so that the induced magnetic field is neglected. No electric field is assumed to be small so that the induced magnetic field is neglected. Under these assumptions, along with the Boussinesq approximations, the boundary layer equations for this problem can be written as:

$$\frac{\partial u}{\partial x}+\frac{\partial v}{\partial y}=0 \tag{1}$$

$$u\frac{\partial u}{\partial x}+v\frac{\partial v}{\partial y}=\nu\frac{\partial^2 u}{\partial y^2}+g\,\beta\left(T-T_\infty\right)-\frac{\sigma B_0^2}{\rho}u \tag{2}$$

$$u\frac{\partial T}{\partial x}+v\frac{\partial T}{\partial y}=\alpha\frac{\partial^2 T}{\partial y^2}+\frac{\beta^* u}{\rho C_P}\left(T_\infty-T\right)+\frac{Q_0}{\rho C_P}\left(T-T_\infty\right)-\frac{1}{\rho C_P}\frac{\partial q_r}{\partial y} \tag{3}$$

where, x, y are the vertical and horizontal directions, respectively, u, v and T are the fluid velocity component in the x and y directions and temperature, respectively, ρ is the fluid density, ν is the kinematic viscosity , C_P is specific heat at constant pressure, $\alpha\left(K/\rho C_P\right)$ is the thermal diffusivity, K_t is the fluid thermal conductivity, β is the volumetric expansion coefficient, σ is the electric conductivity, B_0 is applied magnetic induction, g is the gravitational acceleration, q_r is the thermal radiation and T_∞ is the free stream temperature. Using the radiative heat flux q_r as given by[16]

$$q_r=-\frac{4\sigma^*}{3K^*}\frac{\partial T^4}{\partial y} \tag{4}$$

where σ^* is the Stefan-Boltzmann constant and K^* is the mean absorption coefficient.
By employing equation (4), Equation (2) becomes:

$$u\frac{\partial T}{\partial x}+v\frac{\partial T}{\partial y}=\alpha\frac{\partial^2 T}{\partial y^2}+\frac{\beta^* u}{\rho C_P}\left(T_\infty-T\right)+\frac{Q_0}{\rho C_P}\left(T-T_\infty\right)+\frac{16a^*T_\infty^3}{3\rho C_P K^*}\frac{\partial^2 T}{\partial Y^2} \tag{5}$$

and the boundary conditions can be written as:

$$\begin{aligned} &u(x,0)=ax, \quad v(x,0)=v_w, \quad T(x,0)=T_w(x)=T_\infty+A_0x, \\ &u(x,\infty)=0, \qquad T(x,\infty)=T_\infty \end{aligned} \tag{6}$$

where, a is a constant, $(v_w < 0)$ is the wall suction, and $(v_w > 0)$ the wall suction for injection, and $T_w(x)$ is the wall temperature. Using the stream function ψ such that

$$u = \frac{\partial \psi}{\partial y}, \quad v = -\frac{\partial \psi}{\partial x} \qquad \textbf{and} \qquad \psi = \sqrt{\nu a}\ \ x f(\eta), \quad \eta = \sqrt{\frac{a}{\nu}}\, y, \quad \theta = \frac{T - T_\infty}{T_w - T_\infty}$$

(7)

By substitution from (7) into equations (1-3), we get:

$$f''' + f f'' - (f' - M) f' = -G_r \theta \qquad \textbf{(8)}$$

$$\frac{(N_R + 1)}{P_r}\theta'' + f\theta' - (1 + \delta_x) f' \theta = -\Delta\theta \qquad \textbf{(9)}$$

where, the Hartmann number $M = \left(\sigma / \rho\alpha\right)^{0.5} B_0$, the Grashof number $G_r = g\,\beta(T_w - T_\infty) / \alpha^2 x$, the Prandtl number $P_r = \frac{\nu}{\alpha}$, the thermal radiation parameter $N_R = 16\sigma^* T_\infty^3 / 3K^* K_t$, heat generation $\delta_x = \beta^* x / \rho C_P$, the absorption $\Delta = Q_0 / \rho C_P \alpha$. The appropriate flat plate, free convection boundary condition is also transformed into the applicable form,

$$\begin{aligned} &f'(0) = 1, \quad f(0) = -f_0, \quad \theta(0) = 1, \\ &f'(\infty) = 0, \quad \theta(\infty) = 0 \end{aligned} \qquad \textbf{(10)}$$

where, $f_0 = \frac{v_w}{\sqrt{a\nu}}$ is the wall mass transfer coefficient such that $f_0 < 0$ indicates wall suction and $f_0 > 0$ corresponds to wall blowing conditions.

The resulting differential equations contain arbitrary parameters, the Prandtl number P_r, the magnetic field strength and the buoyant force, the ratio of the Hartmann number is a measure of the relative influence of the magnetic and buoyant forces on the temperature and flow fields. Solution of the resulting semi-infinite domain, nonlinear equations is accomplished with a three part series method. The employed power series, contains a term A that satisfies the boundary conditions and differential equations at infinity, a second term that satisfies the boundary conditions at zero and is the solution to the initial homogeneous differential equation, and additional terms that are utilized to obtain increased numerical accuracy. This accuracy is limited by number of terms that will not initiate divergence of the numerical results:

$$F = A + \varepsilon F_1 + \varepsilon^2 F_2 + \varepsilon^3 F_3 + \cdots \qquad \textbf{(11)}$$

$$\theta = \varepsilon \theta_1 + \varepsilon^2 \theta_2 + \varepsilon^3 \theta_3 + \cdots \qquad \textbf{(12)}$$

$$\begin{aligned} &\eta = 0, \quad F'(0) = 1, \quad F_1(0) = -F_0, \quad F_2(0) = F_3(0) = 0, \\ &\qquad \theta_1(0) = 1, \quad \theta_2(0) = \theta_3(0) = 0 \end{aligned} \qquad \textbf{(13)}$$

$$\eta \to \infty, \quad F_n'(\infty) = F_n(\infty) = 0, \quad F(\infty) = A, \quad \theta_n(\infty) = 0, \qquad n = 1,2,3$$

Equation (12), the temperature representation, along with equation (11) and the associated boundary conditions equation (13), contain an undetermined parameter $\varepsilon \langle\langle 1$ which aids in the collection of terms for each set of the resulting linear differential equations. Substitution of the series representation into the differential equations and collection of terms by like powers of ε result in a family of linear differential equations, and the first three sets are:

$$F_1''' + A F_1''' - M^2 F_1' = -G_r \theta_1 \qquad \textbf{(14)}$$

$$\frac{(N_R+1)}{P_r}\theta_1'' + A\theta_1' + \Delta\theta_1 = 0 \quad \textbf{(15)}$$

$$F_2''' + AF_2'' - M^2F_2' = -F_1F_1''' + F_1'^2 - G_r\theta_2 \quad \textbf{(16)}$$

$$\frac{(N_R+1)}{P_r}\theta_2'' + A\theta_2' + \Delta\theta_2 = -F_1\theta_1' + (1+\delta_x)F_1'\theta_1 \quad \textbf{(17)}$$

$$F_3''' + AF_3'' - M^2F_3' = -F_1F_2'' - F_2F_1'' + 2F_1'F_2' - G_r\theta_3 \quad \textbf{(18)}$$

$$\frac{(N_R+1)}{P_r}\theta_3'' + A\theta_3' + \Delta\theta_3 = -F_1\theta_2' - F_2\theta_1' + (1+\delta_x)(F_1'\theta_2 + F_2'\theta_1) \quad \textbf{(19)}$$

The solutions to the first two sets, Eqs. (20-22), when substituted into Eqs. (11)-(12), provide the required representations for F and θ'. The constant A is determined by satisfying the boundary conditions F(0) and is a function of P_r and M.

$$\theta_1 = e^{-a_1\eta} \quad \textbf{(20)}$$

$$F_1 = -f_0 + a_3\left(e^{a_2\eta} - 1\right) + \frac{G_r\left(e^{-a_1\eta} - 1\right)}{a_1\left(a_1^2 - Aa_1 - M^2\right)} \quad \textbf{(21)}$$

$$\theta_2 = -(a_5 + a_6)e^{-a_1\eta} + a_5e^{(a_2 - a_1)\eta} + a_6e^{-2a_1\eta} + a_7\,\eta\, e^{-a_1\eta} \quad \textbf{(22)}$$

$$F_2 = a_{18} + (a_{17} + a_{92}\eta)e^{a_2\eta} - (a_{13} + a_{16} + a_{94} + a_{93}\eta)e^{-a_1\eta} - a_{14}e^{(a_2 - a_1)\eta} + a_{15}e^{-2a_1\eta} \quad \textbf{(23)}$$

The skin friction coefficient and the wall heat transfer are important physical parameters for this flow and heat transfer situation. Knowing the velocity, we can calculate the skin friction and from temperature field the rate of heat transfer in terms of the Nusselt number

RESULTS AND DISCUSSIONS

For the purpose of discussing the results, some numerical calculations are carried out for non dimensional velocity, surface temperature gradient, skin friction and Nusselt number for different values of heat generation, wall suction/blowing conditions, Grashof number, Hartmann number, Thermal radiation parameter and heat absorption generation.

Table (1): Comparison of the non dimensional wall temperature gradient $(-\theta'(0))$

	$f_0 = 0.45$ $\delta_x = 0.5$	$f_0 = 0.45$ $\delta_x = 1.0$	$f_0 = 0.0$ $\delta_x = 0.5$	$f_0 = 0.0$ $\delta_x = 1.0$
Acharya et al [23]	**0.8225**	**0.9618**	**0.9462**	**1.0789**
Chamkha [12]	**0.82397**	**0.96191**	**0.94769**	**1.07996**
Present work	**0.822757**	**0.9626045**	**0.946481**	**1.077021**

Figs. (1) and (2) illustrate the non dimensional wall temperature gradient $(-\theta'(0))$ against magnetic parameter M for various values of the suction or injection parameter f_0 and the heat generation or absorption parameter δ_x. It can be noted that, the effect of the suction parameter is to

reduce the temperature field while the injection parameter increases it. Figs 1 and 2 show that the non dimensional wall temperature gradient $(-\theta'(0))$ increases as δ_x increases.

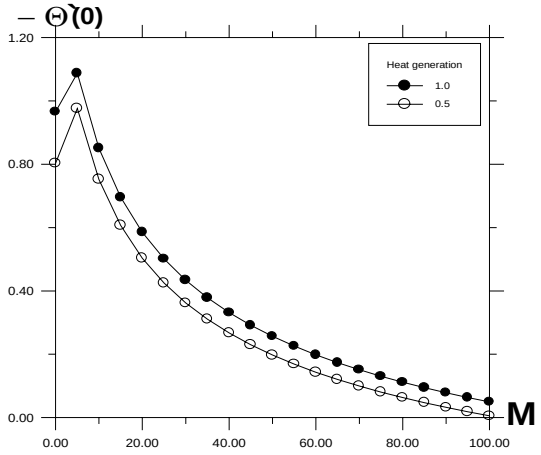

Fig. (1): Variation of non dimensional wall temperature gradient $(-\theta'(0))$, for different values of heat generation, when Pr = 0.71, $G_r = 0.0$, $f_0 = 0.45$, $N_R = 0.0$, $\Delta = 0.0$, $\eta = 1.0$

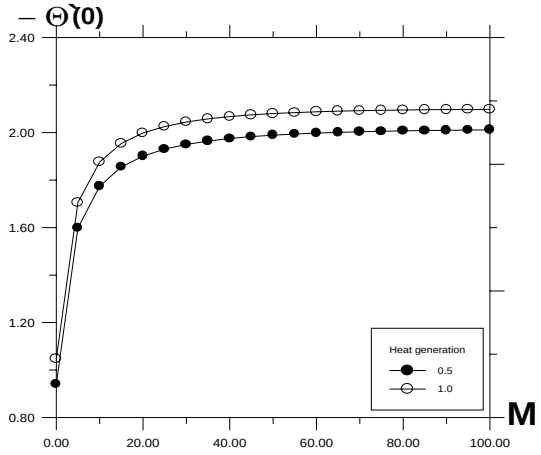

Fig. (2):. Variation of non dimensional wall temperature gradient $(-\theta'(0))$, for different values of heat generation, when $P_r = 0.71$, $G_r = 0.0$, $f_0 = 0.0$, $N_R = 0.0$, $\Delta = 0.0$, $\eta = 1.$

Figs. (3) and (4) illustrate the variations f_0, M and N_R on the wall velocity $-f''(0)$. As mentioned before increasing the value of the suction, injection parameter f_0 causes both the hydrodynamic and thermal boundary layers to increase causing the wall gradients of the velocity profile to decrease.

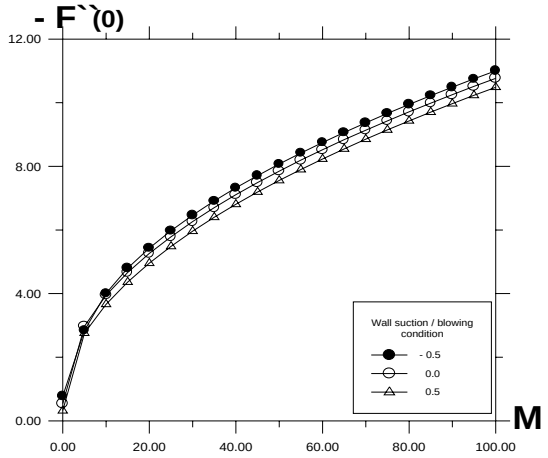

Fig. (3):. Variation of non dimensional surface velocity gradient $(-f''(0))$, for different values of wall suction blowing (f_0), when P_r = 0.71, G_r **= 1.0,** δ_x **= 0.0,** N_R **= 0.0,** $\Delta = 0.0$, $\eta = 1.0$

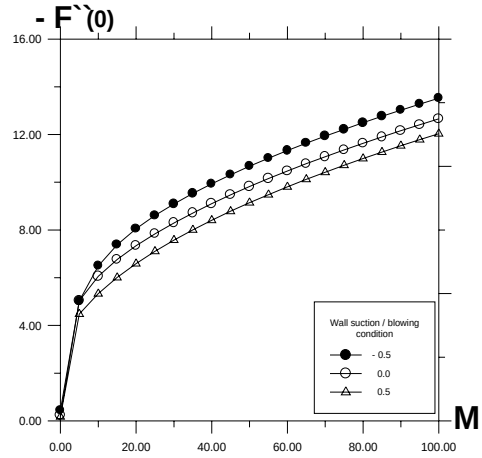

Fig. (4):. Variation of non dimensional surface velocity gradient $(-f''(0))$, for different values of wall suction blowing (f_0), when P_r = 0.71, G_r **= 1.0,** δ_x **= 0.0,** N_R **= 5.0,** $\Delta = 0.0$, $\eta = 1.0$

To see the effect of inclusion of Grashof number (G_r) on the boundary layer flow, in Figs. (5) and (6), the non dimensional velocity $f'(\eta)$ and the non dimensional temperature $\theta(\eta)$ are plotted against η and different values of (G_r), respectively. All of the parameters for the other effects are set to zero in order to study the influence of a single effect at a time. Increases in the values of Grashof number have the tendency ti induce more flow in the boundary layer due to the effect of the thermal buoyancy. For small buoyancy effects (G_r = 1.0), the maximum flow velocity occurs at the surface.

However, as the buoyancy effect get relatively large, a distinctive peak in the velocity profile occurs in the fluid adjacent to the wall and this peak becomes fluid adjacent to the wall and this peak becomes more distinctive as (G_r) increases further.

Along with this flow behavior, the thermal boundary layer reduces as (G_r) increases causing the fluid temperature to reduce at every point other than that of the wall. These flow and thermal behaviors are illustrated by the respective increases and decreases in the velocity and temperature fields as (G_r) increases shown in Figs. 5 and 6.

In addition, the curves show that the peak value of velocity increases rapidly near the wall of the plate as Grashof number increases, and then decays to the relevant free stream velocity.

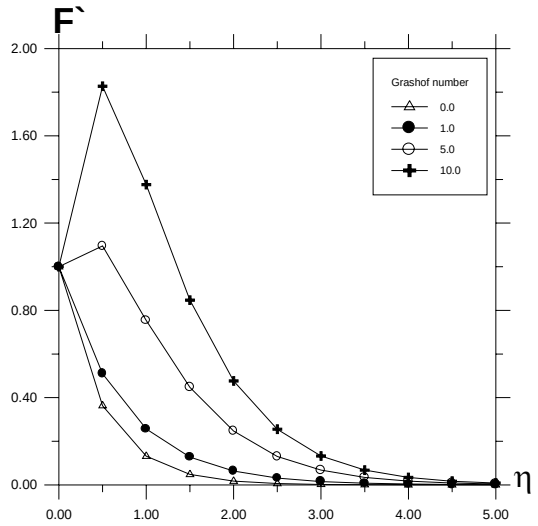

Fig. (5):. Variation of non dimensional velocity $f'(\eta)$ for different values of Grashof number(G), when P_r = 0.71, $F_0 = 0.0$, $\delta_x = 0.0$, $N_R = 5.0$, $\Delta = 0.0$, $M = 0.0$

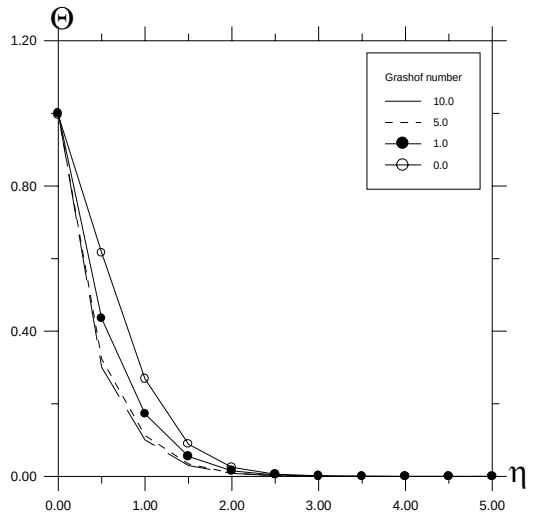

Fig. (6):. Variation of non dimensional temperature $\theta(\eta)$ for different values of Grashof number (G), when P_r = 0.71, F_0 = 0.0, $\delta_x = 0.0$, $N_R = 5.0$, $\Delta = 0.0$, $M = 0.0$

To see the effect of inclusion of magnetic field on the boundary layer flow, in Fig. (7), the non dimensional velocity $f'(\eta)$ is plotted against η for various values of magnetic parameter (M). We observe that the effect of magnetic field is to decrease the velocity as well as the boundary layer thickness. Application of a transverse magnetic field to an electrically conducting fluid gives rise to a resistive type force called the Lorentz force.

This force has the tendency to slow down the motion of the fluid in the boundary layer and to increase its non dimensional temperature. Also, the effects on the flow and thermal fields become more so as the strength of the magnetic field increases.

This is obvious from the decreases in the velocity distributions and the increases in the non dimensional temperature distributions presented in Figs. (7) and (8). Application of a transverse magnetic field normal to the flow direction gives rise to a resistive drag like force acting in a direction opposite to that of flow.

This has a tendency to reduce the fluid tangential velocity and increase its temperature. This is indicative from the decreases and increases in u and θ as M increases shown in Figs. 7 and 8, respectively.

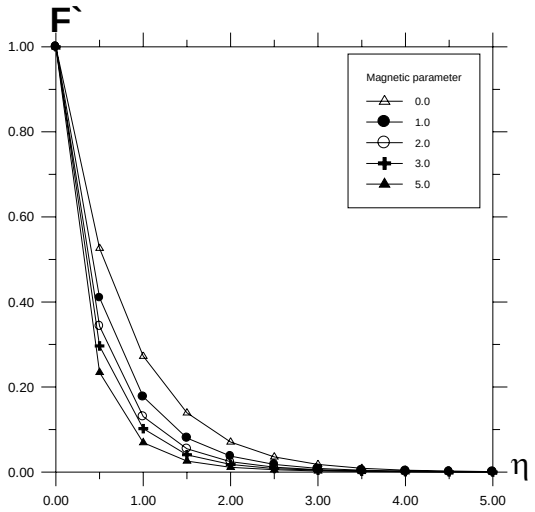

Fig. (7):. Variation of non dimensional velocity $f'(\eta)$ for different values of magnetic parameter, when $P_r = 0.71$, $F_0 = 0.0$, $\delta_x = 0.0$, $N_R = 0.0$, $\Delta = 0.0, G = 1.0$

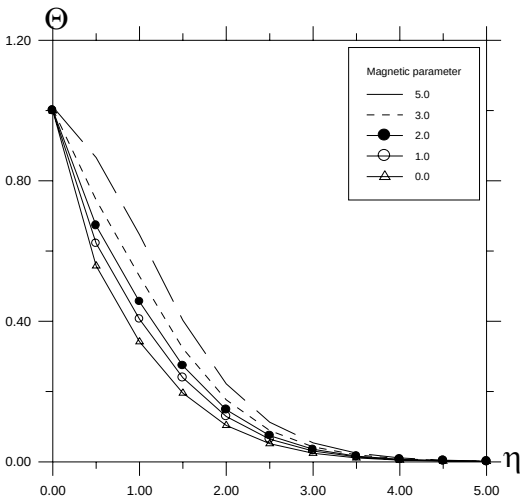

Fig. (8):. Variation of non dimensional temperature $\theta(\eta)$ for different values of magnetic parameter, when $P_r = 0.71$, $F_0 = 0.0$, $\delta_x = 0.0$, $N_R = 0.0$.

Figs. (9) and (10) are the graphical representation of horizontal velocity profile $f'(\eta)$ and temperature profile $\theta(\eta)$ against η for different values of the thermal radiation parameter N_R, respectively. Increasing the thermal radiation parameter N_R produces significant increases in the thermal condition of the fluid and its thermal boundary layer.

Through the buoyancy effect, this increase in the fluid temperature induces more flow in the boundary layer causing the velocity of the fluid there to increase. In addition, the hydrodynamic boundary layer thickness increases as a result of increasing N_R .

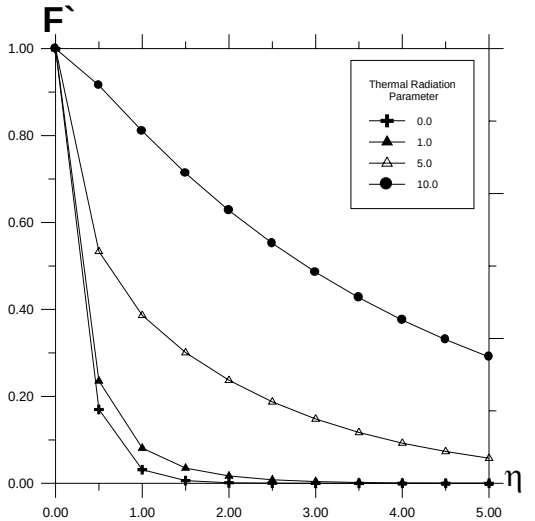

Fig. (9):. Variation of non dimensional velocity $f'(\eta)$ for different values of thermal radiation parameter, when $P_r = 0.71$, $F_0 = 0.0$, $\delta_x = 0.0$, $G = 1.0$, $\Delta = 0.0$

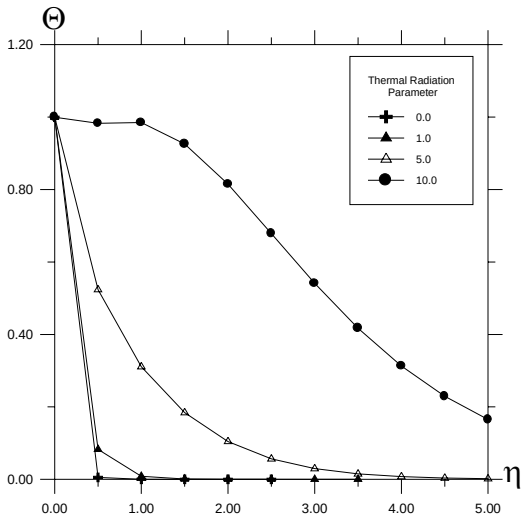

Fig. (10). Variation of non dimensional temperature $\theta(\eta)$ for different values of thermal radiation parameter when, $P_r = 0.71$, $F_0 = 0.0$, $\delta_x = 0.0$, $G = 1.0$, $\Delta = 0.0$

The effect of surface mass transfer f_0 on the dimensionless velocity and temperature distributions are displayed in Figs. (11) and (12). The effect of suction is to make the velocity and temperature distributions more uniform within the boundary layer. It is known that imposition of wall fluid suction reduces both the hydrodynamic and thermal boundary layers which indicate reduction in both the fluid non dimensional velocity and non dimensional temperature distributions. However, the exact opposite behavior is produced by imposition of wall fluid blowing or injection.

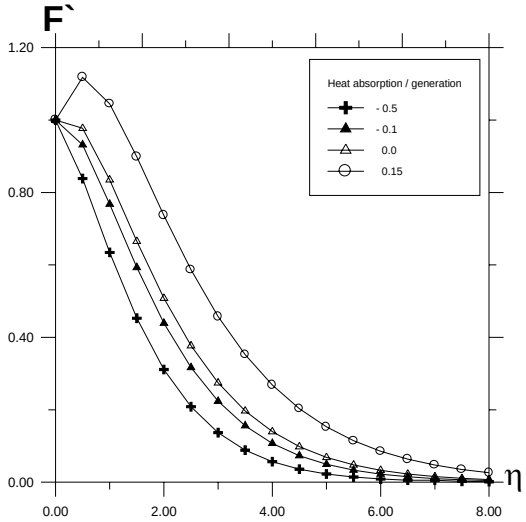

Fig. (11):. Variation of non dimensional velocity for different values of heat absorption /generation parameter when, P_r = 0.71, N_R= 0.0, δ_x = 0.0, G = 1.0, $f_0 = 0.0, M = 0.0$

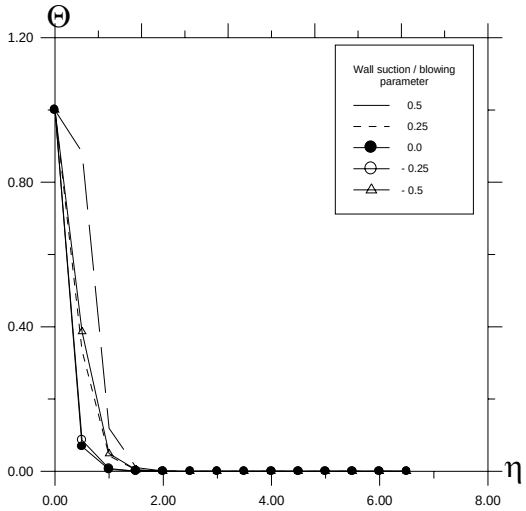

Fig. (12): Variation of non dimensional temperature $\theta(\eta)$ for different values of wall suction / blowing parameter when,. $P_r = 0.71$, $N_R = 0.0$, $\delta_x = 0.0$, G = 1.0, $\Delta = 0.0, M = 0.0$

The influence of the presence of a heat source or a heat sink in the boundary layer on the temperature distribution field is depicted in Fig. (13). The presence of a heat source in the boundary layer generates energy which causes the non dimensional temperature distribution of the fluid to increase. This increase in non dimensional temperature produces on increase in the flow field due to the buoyancy effect. On the other hand, the presence of a heat sink in the boundary layer absorbs energy which causes the non dimensional temperature of the fluid to decrease. This decrease in the fluid non dimensional temperature causes a reduction in the flow velocity in the boundary layer as a result of the buoyancy effect which couples the flow and thermal problems.

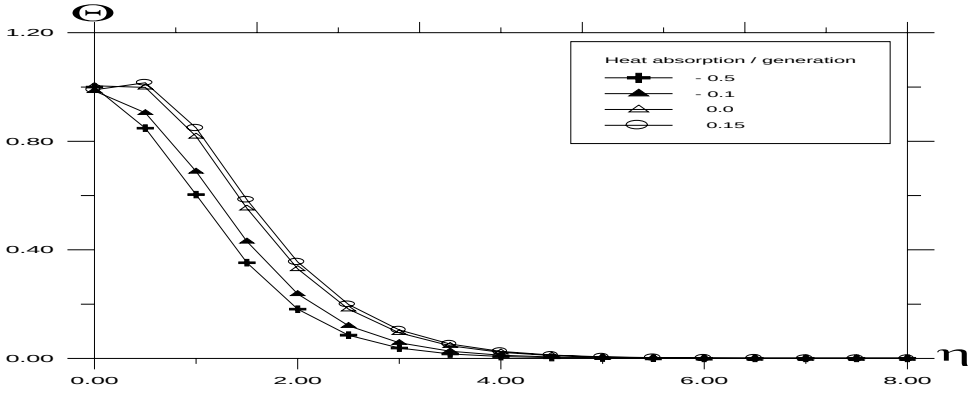

Fig. (13): Variation of non dimensional temperature $\theta(\eta)$ for different values of heat absorption/ generation when, P_r = 0.71, N_R= 0.0, δ_x = 0.0, G = 1.0, $M = 0.0, f_0 = 0.0$

CONCLUSION

The problem considered in this work was that of steady, laminar, viscous boundary layer flow over an accelerating semi infinite porous surface in the presence of a magnetic field, thermal radiation, buoyancy, heat generation or absorption. The coupled nonlinear partial differential equations were solved numerically by perturbation technique. The obtained results were compared with previously work and were found in good agreement. It was found that the wall heat transfer decreases due to the presence of magnetic field, heat generation, thermal radiation or positive wall mass transfer, while it increases by the presence of thermal buoyancy effect.

REFERENCES

(1) J.A. Shercliff "A text book of Magnetohydrodynamic" NY: Pergamon Press Inc.: (1965).
(2) P.C. Ram, S.S. Singh and R.K. Jain ; AstroPhys. Space Sci.; 168, 209(1990).
(3) B.K. Jha and R. Prasad; J. Math. Phys. Sci.; 26(1), 1,(1992).
(4) HS. Takhar, P.C. Ram , Garba EJD and J.K. Bitok ; J. MHD Plasma Res.; 5(2/3), 185 (1995).
(5) DP Georgious and GA. Georgantopoulos ; AstroPhys. Space Sci.; 125, 391 (1986).
(6) V.M. Soundalgekar , JP Bhat and M. Miuddin ; J. Heat Mass Transfer; 9, 199 (1985).
(7) P.C. Ram AstroPhys. Space Sci.; 176, 263, (1991).
(8) N. Chaturuedi , Energy Convers. Mgmt; 38, 1699 (2000).
(9) K. Vajravelu ; Int. J. Eng. Sci.; 35, 1237 (1997).
(10) T.C. Chiam ; Int. J. Eng. Sci.; 33,429, (1995).
(11) I. Pop. and T.Y. Na; Mech. Res. Commun. , 25, 263 (1998).
(12) A.J. Chamkha ; Int. J. of Engineering Science 38, 1699 (2000).
(13) M.M. Abdelkhalek ; Al-Azhar Engineering Fifth International Conference; Vol. 8, P.31-42. Dec. 19-22 (1997),
(14) M.M. Abdelkhalek ; Egypt. J. Phys.; 29, No.1, .39 (1998).
(15) M.M. Abdelkhalek and M.N.H. Comsan ; Egypt. J. Phys., 30, No.1, 107 (1999).
(16) M.M. Abdelkhalek ; Arab J. Nucl. Sci. Appl.; 36(2), 179 (2003).
(17) M.M. Abdelkhalek; Arab J. Nucl. Sci. Appl; 36(2), 189 (2003).
(18) M.M. Abdelkhalek ; Egypt. J. Phys; 34(2), 267 (2003).
(19) M.M. Abdelkhalek ; Arab J. Nucl. Sci. Appl; 37(1), 257-267 (2004).
(20) M.M. Abdelkhalek ; Proceedings of the International Conference on Mathematics Nuclear Physics and Applications in the 21 Century; 479 (Cairo 8-13, March 2003)
(21) HS Takhar , RSR. Gorla and V.M. Soundalgekar; Int. Num. Math. Heat Fluid Flow 77(1996).
(22) E.M.A. Elbashbeshy Can J. Phys.; 78, 1107 (2000).
(23) M. Acharya, L.P. Singh L.P. and G.C. Dash , Int. J. Eng. Sci. 37, 189 (1999)
(24) A. Raptis , Int. J. Heat Mass Transfer 41, 2865 (1998).

APENDIX

$$a_1 = \frac{\left(\frac{AP_r}{N_R+1}\right)+\sqrt{\left(\frac{AP_r}{N_R+1}\right)^2-4\left(\frac{\Delta P_r}{N_R+1}\right)}}{2}, \quad a_2 = \frac{-A-\sqrt{A^2+4M^2}}{2}$$

$$a_3 = \frac{\left(a_1^2-Aa_1-M^2\right)+G_r}{a_2\left(a_1^2-Aa_1-M^2\right)}, \quad a_5 = \frac{(1+\delta_x)a_3a_2+a_1a_3}{\left(\left(a_2-a_1\right)\left(\frac{N_R+1}{P_r}\left(a_2-a_1\right)+A\right)+\Delta\right)}$$

$$a_6 = \frac{-\delta_x G_r}{\left(a_1^2-Aa_1-M^2\right)\left(\frac{4a_1^2\left(N_R+1\right)}{P_r}-2Aa_1+\Delta\right)}, a_7 = \frac{-\left(a_1f_0+a_1a_3+\frac{G_r}{\left(a_1^2-Aa_1-M^2\right)}\right)}{\left(\frac{AP_r}{\left(N_R+1\right)}-2a_1\right)}$$

$$a_8 = -a_3a_2\left(a_2f_0+a_3a_2+\frac{a_2G_r}{a_1\left(a_1^2-Aa_1-M^2\right)}\right),$$

$$a_9 = \frac{-G_r}{\left(a_1^2-Aa_1-M^2\right)}\left(a_1f_0+a_3a_1+\frac{G_r}{\left(a_1^2-Aa_1-M^2\right)}\right), \quad a_{10} = \frac{G_r^2}{\left(a_1^2-Aa_1-M^2\right)},$$

$$a_{11} = \frac{a_3G_r\left(a_1^2+a_2^2\right)}{a_1\left(a_1^2-Aa_1-M^2\right)}, \quad a_{12} = \frac{2a_2a_{13}G_r}{\left(a_1^2-Aa_1-M^2\right)}, \quad a_{13} = \frac{\left(a_5+a_6\right)G_r}{a_1\left(a_1^2-Aa_1-M^2\right)},$$

$$a_{14} = \frac{\left(a_5G_r+a_{11}+a_{12}\right)}{\left(a_2-a_1\right)\left(\left(a_2-a_1\right)^2+A\left(a_2-a_1\right)-M^2\right)}, \quad a_{15} = \frac{G_ra_6}{2a_1\left(4a_1^2-2a_1A-M^2\right)},$$

$$a_{16} = \frac{a_9}{a_1\left(a_1^2-a_1A-M^2\right)}, \quad a_{17} = \left(-a_1a_{13}+a_{14}\left(a_2-a_1\right)+2a_1a_{15}+a_1a_{16}-a_{92}-a_{93}+a_1a_{94}\right)/a_2$$

$$a_{18} = -a_{17}+a_{13}+a_{14}-a_{15}-a_{16}-a_{94}$$

$$a_{92} = \frac{-a_8}{3a_2^2+2Aa_2-M^2}, \quad a_{93} = \frac{a_7G_r}{a_1\left(a_1^2-Aa_1-M^2\right)}, \quad a_{94} = \frac{a_{93}\left(3a_1^2-2Aa_1-M^2\right)}{\left(a_1^2-Aa_1-M^2\right)}$$